

Haverford College

Haverford Scholarship

Faculty Publications

Physics

1974

Laser Heterodyne Study of Water Droplet Growth

Jerry P. Gollub
Haverford College

Ilan Chabay

W. H. Flygare

Follow this and additional works at: https://scholarship.haverford.edu/physics_facpubs

Repository Citation

Gollub, Jerry P., Ilan Chabay, and W. H. Flygare. "Laser heterodyne study of water droplet growth." *The Journal of Chemical Physics* 61.5 (2003): 2139-2144.

This Journal Article is brought to you for free and open access by the Physics at Haverford Scholarship. It has been accepted for inclusion in Faculty Publications by an authorized administrator of Haverford Scholarship. For more information, please contact nmedeiro@haverford.edu.

Laser heterodyne study of water droplet growth

J. P. Gollub, Ilan Chabay, and W. H. Flygare

Citation: *J. Chem. Phys.* **61**, 2139 (1974); doi: 10.1063/1.1682226

View online: <http://dx.doi.org/10.1063/1.1682226>

View Table of Contents: <http://jcp.aip.org/resource/1/JCPSA6/v61/i5>

Published by the [American Institute of Physics](#).

Additional information on *J. Chem. Phys.*

Journal Homepage: <http://jcp.aip.org/>

Journal Information: http://jcp.aip.org/about/about_the_journal

Top downloads: http://jcp.aip.org/features/most_downloaded

Information for Authors: <http://jcp.aip.org/authors>

ADVERTISEMENT



**ALL THE PHYSICS
OUTSIDE OF
YOUR JOURNALS.**

www.physics today.org
**physics
today**

Laser heterodyne study of water droplet growth*

J. P. Gollub

Haverford College, Haverford, Pennsylvania 19041

Ilan Chabay† and W. H. Flygare

Noyes Chemical Laboratory and Materials Research Laboratory, University of Illinois, Urbana, Illinois 61801

(Received 2 May 1974)

Droplet growth by condensation under simulated atmospheric conditions has been studied quantitatively in a diffusion cloud chamber. Droplet size distributions were obtained from heterodyne spectra of scattered laser light. The distributions were typically quite narrow, and the time dependence of the mean radius agrees well with theoretical predictions for supersaturations of 1.02–1.05 in the size range 3–7 μm . Our data indicate no need to postulate very small condensation and thermal accommodation coefficients in contrast to previously published work at higher supersaturations. However, the growth rates are anomalously low at supersaturations less than about 1.015.

I. INTRODUCTION AND THEORY

The nucleation and growth by condensation of micron-sized water droplets is an important process in the life history of clouds, and the resulting droplet populations exert a major influence on the Earth's energy balance and climatic patterns. The kinetics of the growth process has been the subject of numerous^{1–3} theoretical investigations, but until recently there were no accurate experimental studies of the growth process. Vietti and Schuster⁴ recently reported accurate measurements of growth in an expansion chamber, but these measurements were made in supersaturations $S = p/p_e$ (ratio of water vapor pressure to the equilibrium vapor pressure) of 1.49 to 3.45. In this paper we present a study of droplet growth in environments having a supersaturation of 1.01 to 1.05, which is much closer to the range important in the Earth's atmosphere. By using a diffusion chamber operated under steady state conditions, we were able to observe the growth process accurately over time intervals much longer than those that could be achieved with an expansion chamber. The size distribution of the droplets is obtained by a newly developed technique⁵ based on heterodyne spectra⁶ of scattered laser light. Basically, a size-dependent Doppler shift is imparted to the scattered light due to the settling of droplets in the Earth's gravitational field. When this scattered light is mixed with a reference signal derived from a stationary scatterer, an audio-frequency heterodyne spectrum results, manifesting a distribution of Doppler shifts that is directly related to the droplet size distribution.

The growth process is rate limited by the diffusion of water molecules toward the droplet and the conduction of the heat of condensation away from the droplet. Thermal conduction is a more important limiting factor at ambient temperatures above 7 °C, and diffusion is the limiting factor at lower temperatures, since the vapor pressure is decreased. However, these two processes are also influenced by "boundary resistances" to the interchange of molecules and energy. These effects can be described by introducing a condensation coefficient β , the probability that an incident vapor molecule becomes part of the liquid droplet, and a thermal accom-

modation coefficient α , which is the fractional thermalization of energy of an air molecule colliding with a droplet. Of course these parameters, which have microscopic significance, are averages over molecular kinetic energy and angle of incidence. They are not reliably known from independent measurements. One of the goals of the present work is to place limits on these parameters.

Fukuta and Walter² and Carstens and Kassner³ predict a growth law of the following form:

$$r \frac{dr}{dt} = \frac{S - 1 - G(r)}{A + B + r^{-1}(Al_\alpha + Bl_\beta)}, \quad (1)$$

where the parameters are defined below.

The rate of change of the radius r is proportional to $S - 1$ except for a small correction $G(r) = 2\sigma M/\rho_1 RT r$ due to the increased vapor pressure of water over a curved surface relative to a flat one (σ is the surface tension of water, M its molecular weight, ρ_1 the density of the liquid phase, R the gas constant, and T the absolute temperature). Additional corrections to the vapor pressure due to nuclei dissolved in the droplet are negligible for the size range of the present experiment. The parameter $A = L^2 M \rho_1 / KRT^2$ limits the growth rate due to the latent heat of water condensation L , and the thermal conductivity K , of the medium surrounding the droplet. The parameter $B = RT \rho_1 / MD \dot{p}_e$ expresses the effect on the rate of the growth of the diffusion constant D of water in air. The terms involving $l_\alpha = K(2\pi M/RT)^{1/2} [\alpha P_a (C_v + \frac{1}{2} R)]^{-1}$ and $l_\beta = (2\pi M/RT)^{1/2} (D/\beta)$ are significant to the extent that the thermal accommodation coefficient α or condensation probability β differ greatly from unity.⁷ These terms are derived from the boundary conditions at the droplet surface using standard transport theory. In the above definition, M_a , P_a , and C_v are the molecular weight of air, the atmospheric pressure, and molar heat capacity of air at constant volume. The theory outlined above could be incomplete if, for example, the nuclei are more influential in this size range than we have assumed. More significantly, the importance of the terms in α and β is not known.

We proceed to a discussion of the cloud chamber and optical heterodyne technique in Secs. II and III, followed

by presentation of observed size distributions and growth curves in Sec. IV, and an evaluation of the results in Sec. V.

II. CLOUD CHAMBER

In order to work at low supersaturations, a cylindrical diffusion chamber with warm saturated upper surface and cool saturated lower surface was chosen (see Fig. 1). If the height of the chamber is much less than its diameter, linear gradients of water vapor pressure and temperature develop, and the supersaturation as a function of height y (where the temperature is T) can be shown to be given by⁹

$$S(y) = \left(\frac{T(y) - T_2}{T_1 - T_2} \right) \left(\frac{P_1 - P_2}{P_e(T)} \right) + \frac{P_2}{P_e(T)} \quad (2)$$

In this expression T_1 and P_1 are the temperature and vapor pressure at the top of the chamber, and T_2 and P_2 the corresponding values at the bottom. Our chamber is 3.5 cm high (between the wire screens) and 10 cm in diameter. The supersaturation $S(y)$ is unity at the top and bottom screens and peaks somewhat below the center. Temperatures at the wire screens were measured with thermocouples to an accuracy of 0.1 K. The temperature along the side wall, which is harder to measure, was found to vary linearly with height to within 10% of the total temperature difference.

The presence of the cylindrical walls introduces a complication because condensation causes S to be unity on the walls. As a result, the vapor pressure does not vary linearly with height. Since we must know $S(y)$ accurately along the vertical axis of the chamber in order to study droplet growth, we determine the effect of wall condensation as follows. The vapor pressure satisfies Laplace's equation in the steady state, the solutions to which are zonal harmonics when expressed in spherical coordinates (r^*, θ, ϕ) with the origin at the center of the chamber. These are

$$Z_l = (r^*)^l P_l(\cos\theta),$$

where $P_l(\cos\theta)$ are Legendre polynomials. A series solution was constructed to eighth order (odd orders except for the first one do not enter), and the coefficients determined which gave a least squares fit to a large number of points on the boundaries, where the vapor pressure is equal to the equilibrium value at the corresponding temperature. This method yielded a good fit

with the worst deviation being 0.1% at the top and bottom perimeters. The vapor pressure at the center was the same for sixth- and eighth-order approximations and was independent of the number of boundary points used. We found that along the axis of the chamber, $[S(y) - 1]$ is 0.94 times that given by Eq. (2) as a result of condensation on the walls. This correction is the same at all heights and is independent of the temperature difference between the screens over the range of these experiments. The accuracy of this correction is limited mainly by our ability to check the temperature linearity at the side walls. We estimate that the maximum possible error in $(S - 1)$ is about 4% of $(S - 1)$, after the above correction has been made.

Another factor that might possibly affect $S(y)$ is a gradual flow of air from top to bottom (see Fig. 1), the purpose of which was to replace condensation nuclei that rain out. However, this flow was so slow that the chamber air was replaced in about 17 min, a time long compared to that required for the establishment of equilibrium vapor pressure and temperature profiles. This air was saturated at the temperature T_1 before entry into the chamber. Finally, we have used double windows and carefully insulated the chamber to prevent heat leaks that might cause convection.

In the steady state operation of the chamber, droplets nucleate near the top of the chamber, grow, and fall through a sequence of known environments at a speed given by the sum of the mean flow speed of the air (6×10^{-5} m/sec) and the Stokes law velocity $v = 2r^2 \rho_1 g / 9\eta$, where g is the gravitational acceleration and η the viscosity of air. The size distribution $N(r)$ was measured as a function of height in the chamber. Measurements made high in the chamber correspond to early times, while measurements made lower correspond to later times in the growth process. In this manner, we can study a transient growth process by a steady state experiment. Each measurement can then take arbitrarily long, since the size distribution at a given height is constant.

The condensation nuclei used in this experiment were those of ambient air, collected in advance so that the population of nuclei was invariant during the course of the experiment. The nuclei are small compared to the droplet sizes under investigation and presumably have little effect on the growth process beyond providing a droplet population that is not completely uniform in size

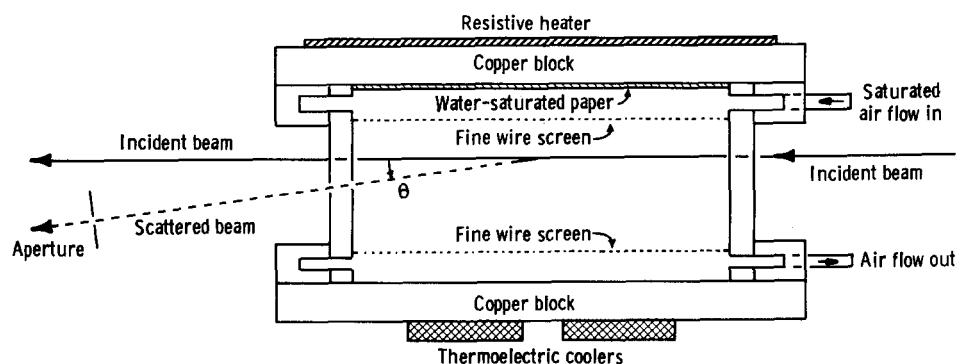


FIG. 1. Side view of the cloud chamber and optical path. The inner dimensions of the chamber are 3.5 cm high (between the screens) by 10 cm diam. A very slow flow of saturated air through the chamber replaces nuclei that rain out. The chamber can be moved vertically with respect to the incident beam in order to measure the droplet size distribution as a function of height.

even near the top of the chamber.

III. LASER HETERODYNE METHOD

Since we have reported elsewhere⁵ the light scattering technique used to obtain the droplet size distribution as a function of height in the chamber, we will simply summarize the method here, together with a few recent changes.

An unfocused (1 mm diam) 150 mW beam from an argon ion laser (with wavelength $\lambda = 5145 \text{ \AA}$ in air) passes horizontally through the chamber, and light scattered at $\theta = 7^\circ$ downward from the horizontal enters the detection system. A 1 mm aperture 66 cm from the center of the chamber limits the observed scattering volume to a rod the diameter of the laser beam and 2 cm long. This scattering volume of 0.02 cm^3 rarely contains more than one droplet at a time, but in several minutes, 25–200 droplets may pass through this region. A final 100 \mu m aperture in front of the EMI 9502 photomultiplier restricts the exposed region to one coherence area. The reference signal for the light beating process was obtained from stray light scattered by the chamber walls and windows.¹⁰ Real time spectrum analysis of the photocurrent fluctuations was obtained from a Federal Scientific UA-14 analyzer and 1015 averager.

The Doppler shift imparted to the light by a droplet moving vertically at speed v_r is

$$\omega_r = (2\pi v_r / \lambda) \sin \frac{1}{2} \theta.$$

We assume that Brownian motion of the droplets is slow compared to v_r , which is a good approximation for droplets larger than about 2 \mu m in radius.⁵ Then the number of droplets of size r_ω (having Doppler shift ω) is related to the photocurrent power spectrum $P(\omega)$ by⁵

$$N(r_\omega) \propto r_\omega P(\omega) / [i_{LO} \langle i_s(r_\omega) \rangle]. \quad (3)$$

Here i_{LO} is the photocurrent due to the local oscillator or reference signal alone, and $\langle i_s(r_\omega) \rangle$ is the mean photocurrent produced by a droplet of size r in the absence of the local oscillator. The latter quantity is proportional to the Mie scattering intensity¹¹ for size r at the angle θ . This quantity is shown in Fig. 2 for $\theta = 7^\circ$ and vertically polarized incident light, as obtained numerically. Since $\langle i_s(r_\omega) \rangle$ has strong oscillations, $P(\omega)$ manifests dips when the size distribution is broad enough to encompass at least one minimum in $\langle i_s(r_\omega) \rangle$. These dips can be used as size markers to check the calibration of the system. Physically, the dips result from the fact that droplets of certain sizes (and corresponding Doppler shifts) scatter little light.

IV. RESULTS

Sample heterodyne spectra are shown in Fig. 3 for three closely spaced heights in the chamber. The dip at 530 Hz is due to a dip in the Mie scattering intensity at 4.24 \mu m (see Fig. 2). Note that the spectral peak shifts to higher frequencies as one observes lower portions of the chamber, indicating the expected increase in size and velocity. However, the Mie scattering dip always remains at the same frequency, as expected. This phenomenon has been observed at several different heights

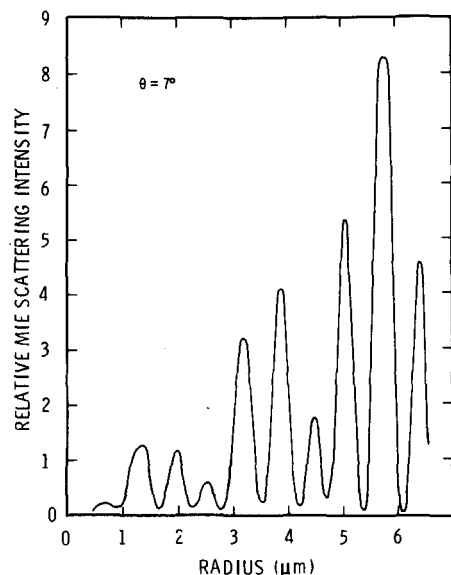


FIG. 2. Scattering intensity at an angle $\theta = 7^\circ$ (for light polarized in the scattering plane) as a function of droplet radius, as calculated from the Mie theory. The normalization is not important for the purposes of this experiment.

with the dips always occurring at the expected frequencies to within 25 Hz, indicating that radii are being measured to an accuracy of about 0.08 \mu m in the range $3\text{--}8 \text{ \mu m}$.

The size distribution corresponding to the middle curve of Fig. 3 has been obtained by applying Eq. (3), and the result is displayed in Fig. 4. The shoulder on the high side of the distribution may be an artifact. The reason for this is that any loss of resolution in the experimental spectra (for example, due to Brownian motion) will cause spurious structure to be introduced into the size distribution when the division of Eq. (3) is performed. However, the most important feature of the distribution is that it is quite narrow compared to the mean radius of 4.20 \mu m , as is always the case for the results reported in this paper. In fact, some of the observed width reflects growth of droplets during their passage through the finite width of the laser beam, so the actual distribution may be even more nearly uniform in size than is apparent from Fig. 4. Therefore it should be meaningful to compare the predictions of Eq. (1) with the observed evolution of the mean radius.

The mean radius at each height was estimated directly from the corresponding heterodyne spectrum. Equation (3) was used only to verify that the distribution was narrow, as discussed above. The Mie scattering curve, which weights the spectrum, introduced some nonsystematic error into the estimation of the mean radius, which limited the precision to 0.1 \mu m in any instance. This limit on the precision is verified by the scatter in the data discussed below, which is on the order of 0.1 \mu m . Systematic error arises from the dependence of the frequency shift on the square of the radius, which means that the root-mean-square radius, rather than the mean radius, was used. The difference between these measures of the radius is 0.03 \mu m typically, which is negligible. A third possible source of error is the distortion

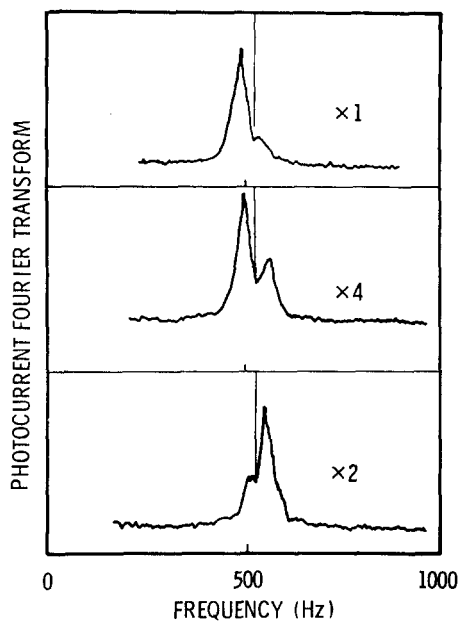


FIG. 3. Square root of the photocurrent power spectrum $P(\omega)$ (or the absolute magnitude of the photocurrent Fourier transform) as traced directly from the output of the spectrum analyzer. The three curves correspond to light scattered by droplets at three heights in the chamber ($y=2.75$, 2.65 , and 2.60 cm, respectively). The spectrum shifts to higher frequencies as one moves lower in the chamber, but the dip, which results from a minimum in the scattering intensity at $r=4.24 \mu\text{m}$, remains at the same frequency. These spectra must be squared to obtain the power spectrum $P(\omega)$ of Eq. (3). The numbers indicate relative gains.

of the spectrum due to droplet growth in the scattering volume, but this contributes much less than $0.1 \mu\text{m}$ to the uncertainty.

The mean radius is plotted as a function of height in the chamber for various temperature differentials in Figs. 5–7, with error bars reflecting the precision of the measurements. The corrected supersaturation profile is also plotted in each case as $100(S-1)$. The theoretical curves were obtained by numerical integration of

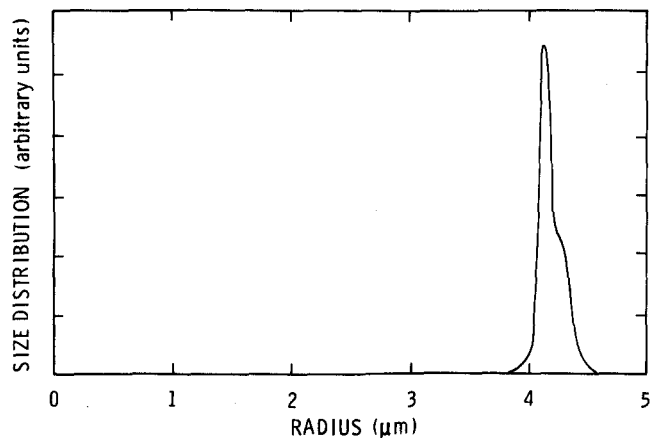


FIG. 4. Size distribution of cloud droplets obtained from the middle spectrum of Fig. 3 by applying Eq. (3). The narrowness of the distribution justifies our subsequent comparison of the growth theory with the evolution of the mean radius.

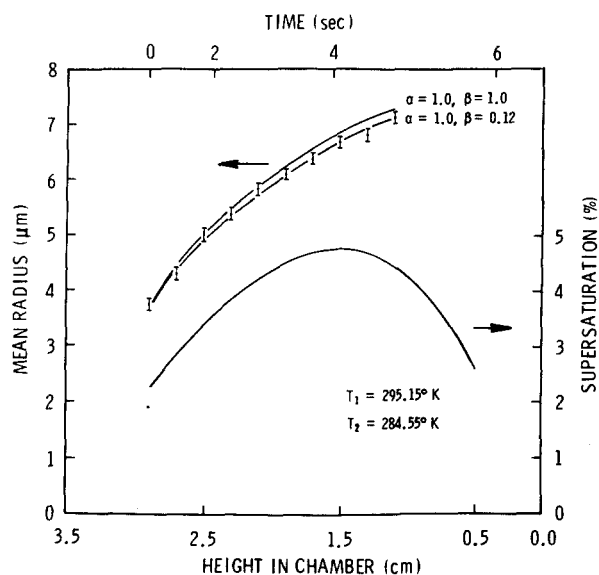


FIG. 5. Mean radius of droplets as a function of height in the chamber when the maximum of $100(S-1)$ (which is also given as a function of height in the lower curve) is 4.7 . The numerically evaluated prediction of the growth theory is given for several choices of thermal accommodation and condensation coefficients α and β . The approximate time scale at the top of the graph was also obtained from the theory.

Eq. (1) with initial conditions appropriate to the highest observable point¹² in the chamber. The fact that the supersaturation and temperature experienced by the droplets as they fall are constantly changing is included in the calculation. The parameters used in the calculation that can significantly affect the results are listed in Table I. The thermal conductivity and diffusion constant are somewhat temperature dependent, but the temperature range to which the droplets are subjected is so narrow that a maximum error of only about 1% in growth rates results from neglecting this temperature dependence. The viscosity is used both for measuring the mean radius and for evaluating the growth theory. Thus,

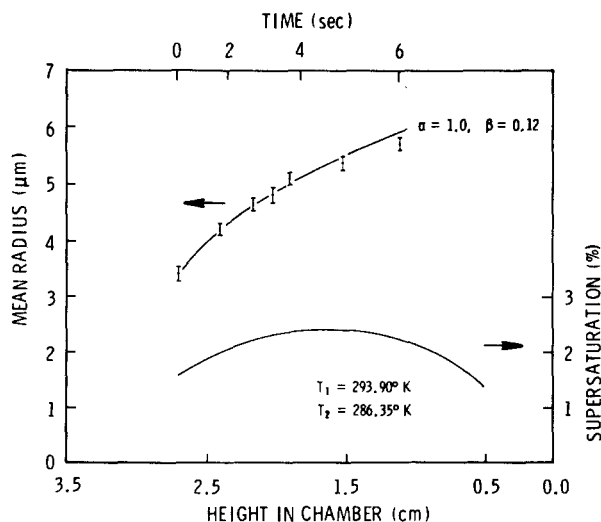


FIG. 6. Same as Fig. 5, except that $100(S-1)$ as shown in the lower curve is less. The theory is plotted for $\alpha=1.0$, $\beta=0.12$, which also gives a good fit to the data of Fig. 5.

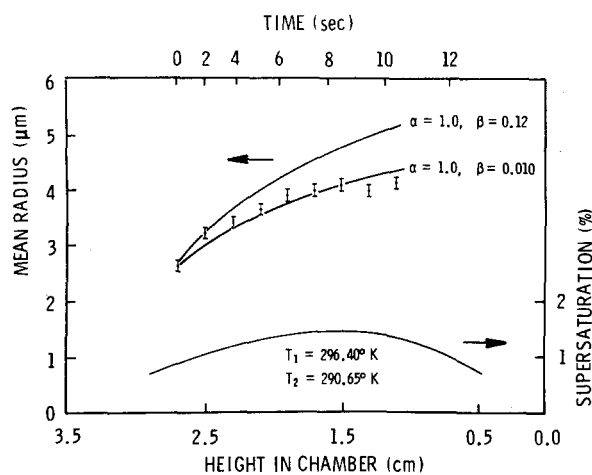


FIG. 7. Same as Fig. 5, except that 100(S-1) never exceeds 1.5 (lower curve). The data in this case are in strong disagreement with the $\alpha = 1.0$ and $\beta = 0.12$ curve that adequately describes the data of Figs. 5 and 6.

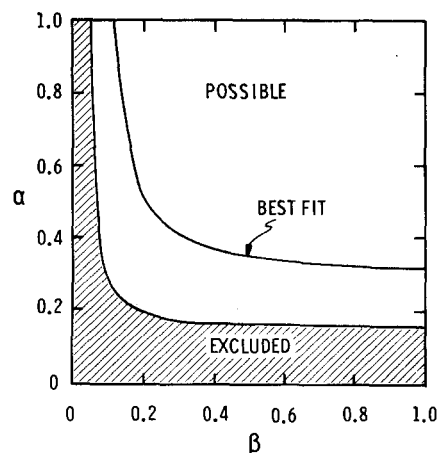


FIG. 8. The values of α and β that are inconsistent with the data of Figs. 5 and 6 lie in the shaded region of this graph. Pairs α, β lying in the unshaded region are consistent with that data, but those pairs yielding the best fit satisfy the relation $\alpha^{-1} = -0.29\beta^{-1} + 3.5$.

its temperature dependence, which is small (0.25% per degree) will not affect the comparison between theory and experiment. The major source of uncertainty in evaluating the theoretical curves is the 4% uncertainty in (S-1) mentioned previously. The precision in the theoretical curves at the lowest point in the chamber is about $0.1 \mu\text{m}$.

In Fig. 5 predictions are shown for $\alpha = \beta = 1.0$ and for $\alpha = 1.0$ and $\beta = 0.12$. It is evident that the measurements lie slightly below the first of these curves, but that the second yields quite a good fit. Note that either α or β must be far from unity to significantly affect the growth curve. It is not possible to determine both α and β from these measurements. In fact, inspection of Eq. (1) shows that the growth curve will be almost the same for all values of α and β for which $(A I_\alpha + B I_\beta)$ takes on a given value. (This quantity is not quite constant during the growth process due to the pressure dependence of B .) The data of Fig. 5 allow us to place limits on the possible values of α and β , as shown in Fig. 8. The region which is excluded by the measurements is shaded. In this region, α or β (or both) is too small to account for the observed growth rates. The remaining area of the figure represents values of α and β that are consistent with the data of Fig. 5, in the sense of producing theoretical growth curves that lie within the error bars. The line labeled "best fit" in Fig. 8 contains pairs of values for α and β which yield growth curves essentially

identical to the one for $\alpha = 1.0$ and $\beta = 0.12$ shown in Fig. 5. For example, $\alpha = 0.31$ and $\beta = 1.0$ would yield essentially the same growth curves as does $\alpha = 1.0$ and $\beta = 0.12$. This line of best fit in the α, β plot is $\alpha^{-1} = -0.29\beta^{-1} + 3.5$.

The data of Fig. 6, for which the maximum supersaturation was only 1.024 instead of 1.047, also follow reasonably well the growth curve for $\alpha = 1.0$, $\beta = 0.12$ (and equivalent pairs). However, the data shown in Fig. 7, for a maximum supersaturation of 1.014, fall consistently below this growth curve. Even a choice of parameters such as $\alpha = 1.0$ and $\beta = 0.010$ produces a relatively poor fit, besides being in the "excluded region" of α, β . Apparently, the droplets essentially cease growing although the surrounding supersaturation is still substantial.

V. DISCUSSION AND CONCLUSIONS

There have been some measurements⁴³ of β for water molecules impinging on ice at cryogenic temperatures indicating a value very near unity ($\beta \geq 0.99$). It is rather difficult to measure β for liquid water directly and reliably, but the large binding energy (compared to thermal energies) suggests that β is not likely to be strongly temperature dependent. Consequently, we feel it is more reasonable to regard the marginally detectable deviations from $\alpha = \beta = 1.0$ in Fig. 5 as being due mainly to $\alpha \neq 1$ rather than $\beta \neq 1$, if they are real.

Vietti and Schuster⁴ found at very high supersaturations that the growth theory expressed in Eq. (1) would fit their data best with $\alpha = 0.1$ and $\beta = 0.035$ (and presumably other equivalent pairs). These values are in the excluded region of our Fig. 8. However, the agreement⁴ was actually poor, since the predicted radii were too small at early times and too large at late times. Their measurements extended over a wider size range than ours, but if one examines only the comparable range ($3\text{--}7 \mu\text{m}$), one finds their data would imply even smaller values of α and β than those quoted above. Vietti and Schuster were sensitive to these problems and suggested other theoretical formulations besides the one used here.

TABLE I. Parameters used in the growth theory.

Property ^a	Symbol	Value	Source
Thermal conductivity of air	K	$2.53 \times 10^{-2} \text{ W m}^{-1} \cdot \text{K}^{-1}$	b
Diffusion coefficient	D	$2.40 \times 10^{-5} \text{ m}^2 \text{ sec}^{-1}$	b
Heat of vaporization	L	$2.45 \times 10^6 \text{ J kg}^{-1}$	c
Surface tension	σ	0.0735 J m^{-2}	c
Viscosity of air	η	$1.795 \times 10^{-5} \text{ kg m}^{-1} \cdot \text{sec}^{-1}$	b

^aAll parameters are evaluated at 15°C.

^bAmerican Institute of Physics Handbook (McGraw-Hill, New York, 1972), 3rd. ed.

^cHandbook of Chemistry (Handbook Publishers, Sandusky, Ohio, 1956), 9th ed.

There appears to be a definite contrast between their results and ours. We find that at supersaturations of 1.02–1.05, Eq. (1) is satisfactory, with values of α , β that do not seem physically unreasonable. Vietti and Schuster find that at supersaturations over 1.5 Eq. (1) provides a roughly correct description only with α , β being very small. One possible explanation is that the rapid time scale of their experiment makes thermal equilibration less complete, but on the other hand the thermal time constant of a 3 μm droplet is only 2×10^{-3} sec.

We do not understand why our data at $1.02 < S < 1.05$ are in better agreement with the theory than the data at $S = 1.01$. If the supersaturation were less than the indicated value, the data for $S > 1.02$ should also be affected. In addition, this hypothesis would not explain the cessation of growth (Fig. 7) in the center of the chamber where the supersaturation is surely the greatest. Vapor depletion is not a possibility at the droplet densities of these experiments.

Another possible explanation of the data at the lowest peak supersaturations is that the nuclei or surface contaminants are substantially affecting the growth process. On the one hand, such effects normally would be expected to increase the growth rates by reducing emission rates of molecules from the surface. On the other hand, there are experiments¹⁴ indicating enhanced molecular emission from contaminated surfaces. In any case, there is no compelling reason why effects of nuclei or surface materials would not be manifested at higher supersaturations as well, if they exist at all. We feel that it will be necessary to study growth on well characterized nuclei in order to understand the low growth rates of Fig. 7. One of us (J. P. G.) is undertaking this work at the present time.

In conclusion, we have observed droplet growth in the 3–7 μm radius range in supersaturations similar to relevant atmospheric conditions for droplet formation. A theoretical description that takes into account imperfect condensation and thermal accommodation at the droplet surface is in good accord with the data for $1.02 < S < 1.05$. The optimum values of α and β are related by $\alpha^{-1} = -0.29\beta^{-1} + (3.5)_{2,2}$, but $\alpha = \beta = 1.0$ is not definitely excluded. For $S < 1.015$ we observe strong deviations from this theory which are not understood. These deviations could be significant for understanding atmospheric processes.

ACKNOWLEDGMENTS

One of us (J. P. G.) would like to thank John Thorsten-

sen and Craig Brashear for experimental and computational assistance, and William Davidson for helpful discussions.

- *Supported in part by National Oceanic and Atmospheric Administration Grant No. 04-4-022-10 to Haverford College and National Science Foundation Grant NSF-GH-33634 to the Materials Research Laboratory at the University of Illinois.
- †Present address: Analytical Chemistry Division, National Bureau of Standards, Washington, D.C. 20234.
- ¹B. J. Mason, *The Physics of Clouds* (Clarendon, Oxford, 1971), pp. 122–125.
- ²N. Fukuta and L. A. Walter, *J. Atmos. Sci.* **27**, 1160 (1970).
- ³J. C. Carstens and J. L. Kassner, *J. Rech. Atmos.* **3**, 33 (1968).
- ⁴M. A. Vietti and B. G. Schuster, *J. Chem. Phys.* **58**, 434 (1973).
- ⁵J. P. Gollub, Ilan Chabay, and W. H. Flygare, *Appl. Opt.* **12**, 2838 (1973).
- ⁶For a general review of optical heterodyne and homodyne spectroscopy, see H. Z. Cummins and H. L. Swinney, in *Progress in Optics* (American-Elsevier, New York, 1970), Vol. 8.
- ⁷The parameters α and β appearing in this theory differ from the true accommodation and condensation coefficients α' and β' by a factor of 2 when α' and β' are near unity, because the modification of the distribution function by the density gradient near the droplet has been neglected. In fact, $\alpha = \alpha' / (1 - \frac{1}{2}\alpha')$, with a similar expression for β . However, the distinction is unimportant when α or β differ from unity enough to significantly affect the growth rate. Therefore, we have not considered it worthwhile to introduce this complication, and we treat α and β as if they are the actual microscopically significant quantities. A discussion of this effect in the case of β may be found in Ref. 8.
- ⁸L. Monchick and H. Reiss, *J. Chem. Phys.* **22**, 831 (1954).
- ⁹V. K. Saxena, J. N. Burford, and J. L. Kassner, Jr., *J. Atmos. Sci.* **27**, 73 (1970).
- ¹⁰We found that the use of a separate reference obtained by re-directing the transmitted beam back onto the exit window of the cloud chamber, as in Ref. 5, resulted in artificially broadened heterodyne spectra. We do not fully understand why this occurs, but we suspect that dust convecting through the reference beam is the cause. Therefore, we have used stray light as a reference, which has one disadvantage. The reference intensity in our geometry is comparable to but not large compared to the intensity scattered by the cloud. Therefore, the homodyne and heterodyne spectra are comparable in magnitude. Since they are generally well separated in frequency, the presence of a homodyne spectrum is not a problem.
- ¹¹M. Kerker, *The Scattering of Light and Other Electromagnetic Radiation* (Academic, New York, 1969).
- ¹²Geometrical constraints prevent us from measuring closer to the top and bottom of the chamber than is shown in Fig. 5.
- ¹³C. E. Bryson III, V. Cazcarra, M. Chouarain, and L. L. Levenson, *J. Vac. Sci. Technol.* **9**, 557 (1971).
- ¹⁴R. B. Hughes and J. F. Stampfer, Jr., *J. Atmos. Sci.* **28**, 1244 (1971).